

**GENESIS OF LUNAR SEGREGATED AND GRAIN RIMS CONDENSATES.** O. I. Yakovlev<sup>1,2</sup>, M. V. Gerasimov<sup>1</sup>, Yu. P. Dikov<sup>1,3</sup>. Russian Academy of Sci.: <sup>1</sup>Space Research Inst., Profsoyuznaya st., 84/32, Moscow, 117997, yakovlev@geokhi.ru; <sup>2</sup>Vernadsky Inst. of Geochem. and Analytical Chemistry; <sup>3</sup>Inst. of Ore Deposits, Petrography, Mineralogy and Geochemistry; Moscow, Russia.

**Introduction:** Investigation of lunar condensates provides important information about high-temperature modification processes which could form the modern geochemical state of the Moon. Hypervelocity impacts produce condensed segregates and films on various soil grains with global distribution over the lunar surface. Keller and McKay [1] indicated the input of solar wind spattering and impact vaporization in the origin of lunar particles rims. Warren [2] has reported about composition of HASP glasses and condensates which were identified in Apollo 14 regolith breccias 14076. Condensates were discovered in the form of small (<10  $\mu\text{m}$ ) spherules and aggregates and were named - GASP (Gas-Associated Spheroidal Precipitate) condensates. GASP condensates were separated into Fe-rich FeGASP and Si-rich SiGASP condensates. We have compared composition of some grain rims condensates, which were assumed as impact-induced condensates based on deficit of oxygen, and GASP particles with experimental data of Markova et al. [3] on evaporation of aluminum-rich basalt 68415,40 delivered by Apollo-16 with calculations of residua melt and complementary vapor compositions at different temperatures. The aim of our investigation was to relate temperatures and mass losses of basaltic material at different stages of its vaporization with compositions of condensed films and GASP condensates.

**Experiment:** The sample of aluminum-rich basalt 68415,40 (starting composition (wt.%):  $\text{SiO}_2$  45.5;  $\text{TiO}_2$  0.3;  $\text{Al}_2\text{O}_3$  28.7;  $\text{FeO}$  4.3;  $\text{MgO}$  4.4;  $\text{CaO}$  16.4;  $\text{Na}_2\text{O}$  0.4  $\text{K}_2\text{O}$  < 0.1) was evaporated using effusive Knudsen technique with mass-spectrometric analysis of the vapor phase [4]. Experimental setup permitted to measure equilibrium temperature and partial pressure of vapor components over melts in the range of temperature up to  $\sim 2600^\circ\text{C}$ . Peculiarity of the method was the possibility of simultaneous measurement of ion current intensities of the sample and of a standard sample in the same chamber. Temperature of evaporation was measured by pyrometer with accuracy of  $\pm 1^\circ\text{C}$ . Evaporation was performed in a tungsten effusive cell. The sample with a mass of 15 g was placed in Re-cap to reduce direct interaction between the melt and tungsten. Evaporation from a Re-cap sufficiently inhibits reductive action of tungsten. Experiment was performed with stepped increase of temperature by  $\sim 50^\circ\text{C}$ . The duration of each step was  $\sim 15$  min what was necessary to gain all the mass-spectrum range. Stepped heating in experiment permitted to keep mole-

cular outflow regime at given sample mass and optimally decrease duration of the experiment. All the duration of the experiment started at  $T \sim 900^\circ\text{C}$  and to the total sample evaporation was 5-7 hours. Measured partial pressure of components permitted to calculate their velocities of evaporation based on Hertz-Knudsen formula. Velocities of evaporation permitted to calculate chemical composition of residua melts and corresponding vapor at different temperatures and mass loss rates. Composition of residua melts was calculated at all time and temperature intervals until its total escape from the Knudsen cell. Elements masses in the melt residua at each temperature step were recalculated to oxide forms and adjusted to 100%. Chemical composition of the vapor was defined as the difference between starting sample and actual residua melt composition. It was also recalculated to oxides form and adjusted to 100%.

**Experimental results:** Fig. 1 shows refractory ( $\text{CaO} + \text{Al}_2\text{O}_3 + \text{TiO}_2$ ) vs. semi-refractory ( $\text{SiO}_2 + \text{MgO}$ ) elements plot of the vapor phase composition in experiment with Apollo-16 aluminum-rich basalt and compositions of iron-rich (I-R) and amorphous (AM) lunar condensed films [1].

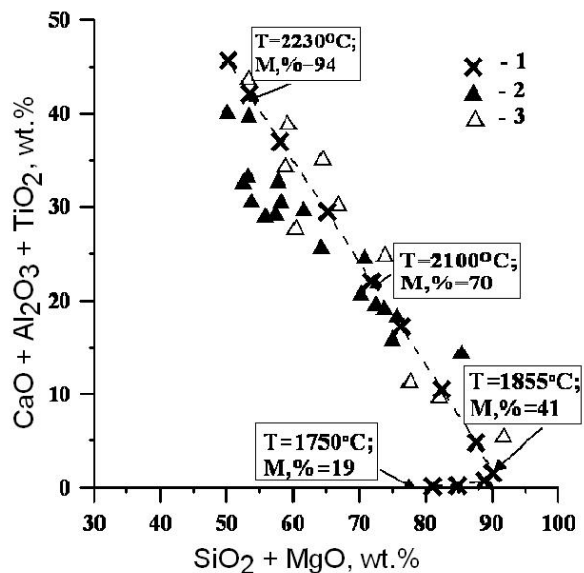


**Fig. 1.** Chemical composition of: 1) - sequential composition of the vapor phase in experiment with the Apollo-16 aluminum-rich basalt (the trend is shown by a dashed line, some points are marked with indication of temperature of the melt (T) and respective mass loss (M)); 2) - iron-rich (I-R) film condensates from [1]; 3) - amorphous (AM) film condensates from [1].

Fig. 2 shows refractory ( $\text{Al}_2\text{O}_3 + \text{CaO}$ ) vs. semi-refractory ( $\text{SiO}_2$ ) and vs. moderately “volatile” ( $\text{FeO}$ ) elements plot with compositions of the vapor from experiment with the Apollo-16 aluminum-rich basalt, FeGASP and SiGASP particles, and lunar grain rims condensates [1]. The turning point at  $\text{SiO}_2$  corner corresponds to  $T \sim 1855^\circ\text{C}$  and  $M, \% = 41$ .

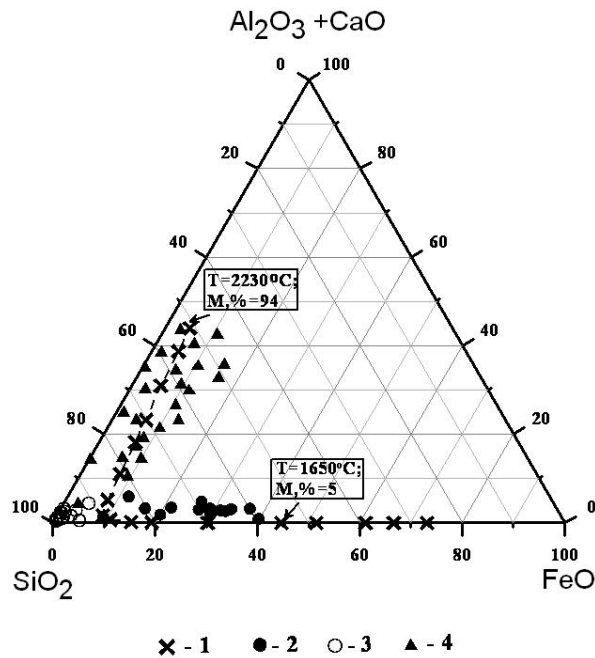


**Fig. 2.** Chemical composition of: 1) - sequential composition of the vapor phase in experiment with the Apollo-16 aluminum-rich basalt (the trend is shown by a dashed line, two points are marked with indication of temperature of the melt ( $T$ ) and respective mass loss ( $M$ )); 2) – FeGASP particles from [2]; 3) – SiGASP particles from [2]; 4) – film condensates (I-R and AM) from [1].

The experiment shows typical row of volatility of elements from basaltic melt:  $(\text{K}_2\text{O} + \text{Na}_2\text{O}) - \text{FeO} - \text{SiO}_2 - \text{MgO} - (\text{CaO} = \text{TiO}_2) - \text{Al}_2\text{O}_3$ . Alkalis are dominant in the vapor (up to 20÷50 wt.%) at temperature range  $\sim 1300\text{--}1550^\circ\text{C}$  and mass loss  $< 2\%$ . Iron is dominant (up to 55%) at 1300 to  $1600^\circ\text{C}$  range and mass loss  $< 5\%$ . Silicon is dominant (up to 85%) in the range 1700 to  $2050^\circ\text{C}$  and mass loss from 15 to 65%.  $\text{MgO}$  is active in the range  $1900\text{--}2000^\circ\text{C}$ . At temperatures  $> 2100^\circ\text{C}$  and mass loss  $> 65\%$   $\text{CaO}$ ,  $\text{TiO}_2$ , and  $\text{Al}_2\text{O}_3$  are dominant. These refractory elements are almost absent in the vapor below  $1850^\circ\text{C}$ .

**Discussion:** It is remarkable that all compositions of condensed lunar findings are correlated with com-

positional evolution of the vapor over basaltic melt within the whole range of its variation. Compositions of different condensed objects reflect composition of the vapor at different stages of its compositional trend.

Fig. 2 shows that all oxygen deficient film condensates correspond to high-temperature ( $1850$  to  $2230^\circ\text{C}$ ) experimental trend. High  $\text{CaO}$  and  $\text{Al}_2\text{O}_3$  concentration is a result of the vapor depletion in higher volatility elements during high temperature stage of vaporization. Fig. 1 also indicates no principal difference in the compositional diversity of I-R and AM film condensates. This speaks for their identical condensational origin.

Individual condensed particles such as FeGASP and SiGASP particles have low concentration of refractory elements (mean concentration of  $\text{Al}_2\text{O}_3$  is  $\sim 0.4$  wt.%). Fig. 2 shows that compositions of FeGASP particles correlate with condensation at temperatures in the range  $1650$  to  $1850^\circ\text{C}$ . More iron enriched FeGASPs were formed at lower temperatures compared to iron-depleted FeGASPs.

SiGASPs have mean concentration of silicon  $\sim 90$  wt.% what is slightly higher than the maximum concentration of Si in the vapor in the experiment ( $\sim 85$  wt.%). Nevertheless, SiGASPs are well on the general trend of compositional change of the vapor, though the effect of  $\text{SiO}_2$  purification is still unclear. Position of SiGASPs on the plot indicates their formation at higher temperatures compared with the same for FeGASPs.

Impact-induced vaporization proceeds at shorter time periods compared to experimental runs. This is provided by a sufficiently higher vapor pressure and respectively higher temperatures. Nevertheless, the sequence of compositional change of the vapor must be about the same. The possible difference in the starting chemical composition of evaporated rocks also does not change the sequence in the compositional change of the vapor but shifts somehow proportions of produced condensates of different types.

**Acknowledgment:** This work was supported by RFBR grant 08-05-00786.

**References:** [1] Keller L.P., McKay D.S. (1997) *GCA*, 61, p. 2331-2341. [2] P. H. Warren (2008) *GCA*, 72, p. 3562-3585. [3] Markova O. M., Yakovlev O. I., et al. (1986) *Geokhimiya*, No 11, p.1559-1569 (in Russian). [4] Semenov G. A., et al. Mass-spectroscopy in Chemistry (1976), L. Nauka. 150 p. (in Russian).